AD-A038 030 HARRY DIAMOND LABS ADELPHI MD F/G 16/3
NASTRAN STRUCTURAL ANALYSIS OF A MISSILE FUZE ELECTRONIC ASSEMB--ETC(U)
DEC 76 D W NEILY
UNCLASSIFIED HDL-TM-76-37 NL

| OF |
AD A038030

END

DATE FILMED
4-77

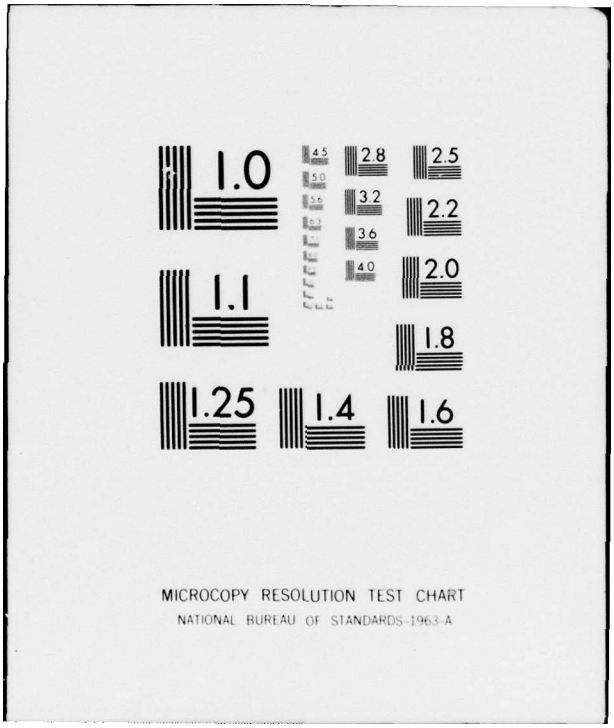
1.0
1.1
1.25
1.4
1.6
1.8
2.0
2.2
2.5
2.8
3.2
3.6
4.0
4.5
5.0
5.6
6.3
7.1
8.0
9.0
MICROCOPY RESOLUTION TEST CHART
NATIONAL BUREAU OF STANDARDS-1963-A

HDL-TM-76-37

NASTRAN Structural Analysis of a Missile Fuze Electronic Assembly

December 1976

U.S. Army Material Development and Readiness Command
HARRY DIAMOND LABORATORIES
Adelphi, Maryland 20783

UNCLASSIFIED

SECURITY CLASSIFICATION OF THIS PAGE *(When Data Entered)*

REPORT DOCUMENTATION PAGE

READ INSTRUCTIONS BEFORE COMPLETING FORM

1. REPORT NUMBER: HDL-TM-76-37	2. GOVT ACCESSION NO.
3. RECIPIENT'S CATALOG NUMBER	
4. TITLE *(and Subtitle)*: NASTRAN Structural Analysis of a Missile Fuze Electronic Assembly.	5. TYPE OF REPORT & PERIOD COVERED: Technical Memorandum
6. PERFORMING ORG. REPORT NUMBER	
7. AUTHOR(s): Darrell W. Neily	8. CONTRACT OR GRANT NUMBER(s): DA 1X364307D212
9. PERFORMING ORGANIZATION NAME AND ADDRESS: Harry Diamond Laboratories, 2800 Powder Mill Road, Adelphi, MD 20783	10. PROGRAM ELEMENT, PROJECT, TASK AREA & WORK UNIT NUMBERS: Program: 6.43.07.A
11. CONTROLLING OFFICE NAME AND ADDRESS: U.S. Army Materiel Dev & Readiness Com, Attn PMO, Patriot, Redstone Arsenal, AL 35809	12. REPORT DATE: Dec[redacted]976
	13. NUMBER OF PAGES: 26
14. MONITORING AGENCY NAME & ADDRESS *(if different from Controlling Office)*	15. SECURITY CLASS. *(of this report)*: UNCLASSIFIED
	15a. DECLASSIFICATION/DOWNGRADING SCHEDULE

16. DISTRIBUTION STATEMENT *(of this Report)*

Approved for public release; distribution unlimited.

17. DISTRIBUTION STATEMENT *(of the abstract entered in Block 20, if different from Report)*

18. SUPPLEMENTARY NOTES

HDL Project: 610661
DRCMS Code: 634307.12.17100

19. KEY WORDS *(Continue on reverse side if necessary and identify by block number)*

Stress	Missile fuze
Structural analysis	Fuze
Vibration	Mode shape
NASTRAN	

20. ABSTRACT *(Continue on reverse side if necessary and identify by block number)*

The structure of the XM818 Fuze Electronic Assembly for application in the Patriot missile was analyzed by using the NASTRAN computer program. The levels and locations of maximum stress were found for a static loading. The shapes and frequencies of the lowest vibration modes were also computed. However, because of several limiting assumptions in the analysis, the stress levels for dynamic loads were not included. Experiments are recommended to obtain this information.

DD FORM 1 JAN 73 1473 EDITION OF 1 NOV 65 IS OBSOLETE

UNCLASSIFIED

SECURITY CLASSIFICATION OF THIS PAGE *(When Data Entered)*

163 050

CONTENTS

FIGURES

FIGURES (CONT'D)

TABLES

1. INTRODUCTION

While the components in today's electronic missile fuzes are generally rugged, they depend on a packaging structure for most of their support. This structure must hold up under the missile flight loads and not substantially amplify them at component mounting points. Since the components may be sensitive to excessive motion, or to oscillation at a particular frequency, the designer of an electronic assembly should seek to isolate or minimize the effects of the harshest environments.

This report describes the structural analysis of a missile fuze electronic package. The package under study, the XM818 Fuze Electronic Assembly (EA) for application in the Patriot missile, was designed from layouts based on experience from similar missile fuze programs. The structural analysis described in this report was conducted afterward to validate the adequacy of the design in terms of maximum stress and lowest resonant frequencies. Although there were no specific requirements, it was desired that the safety factors be larger than 1.25 (a typical figure for unmanned missiles), and that resonant frequencies be higher than 500 Hz (the top of the transportation vibration spectrum). On the other hand, a large safety factor should not be construed as an overdesign. For the most part, the castings were made at the minimum castable thickness.

The XM818 EA is a complex electronic unit of modular subassemblies in a sealed can (fig. 1) that is attached to the missile on four triangular mounting flanges. Three major subassemblies, the receiver, converter, and processor, are affixed to threaded bosses cast in the can. Each subassembly consists of a housing, circuit boards, filters, and other electronic components. Most of the filters and components, and some of the circuit boards are attached to the subassembly structures by screws. The remaining boards are held in place by Birtcher tracks.

The computations were done with the NASTRAN structural analysis computer code.[1] This powerful tool is able to handle fairly complicated analyses that would otherwise be impossible. An analysis for the XM818 EA was considered to be of this type.

The complexity of the geometry and mountings in the EA would have made a straightforward NASTRAN analysis overly difficult and expensive. The fuze housing, for example, is a complex casting and would be time-consuming to model and unwieldy to program. Fortunately, it was possible to analyze the EA in individual reasonably sized substructures, and still obtain important information.

---

[1] *C. W. McCormick, ed., The NASTRAN User's Manual, NASA SP-222 (October 1969).*

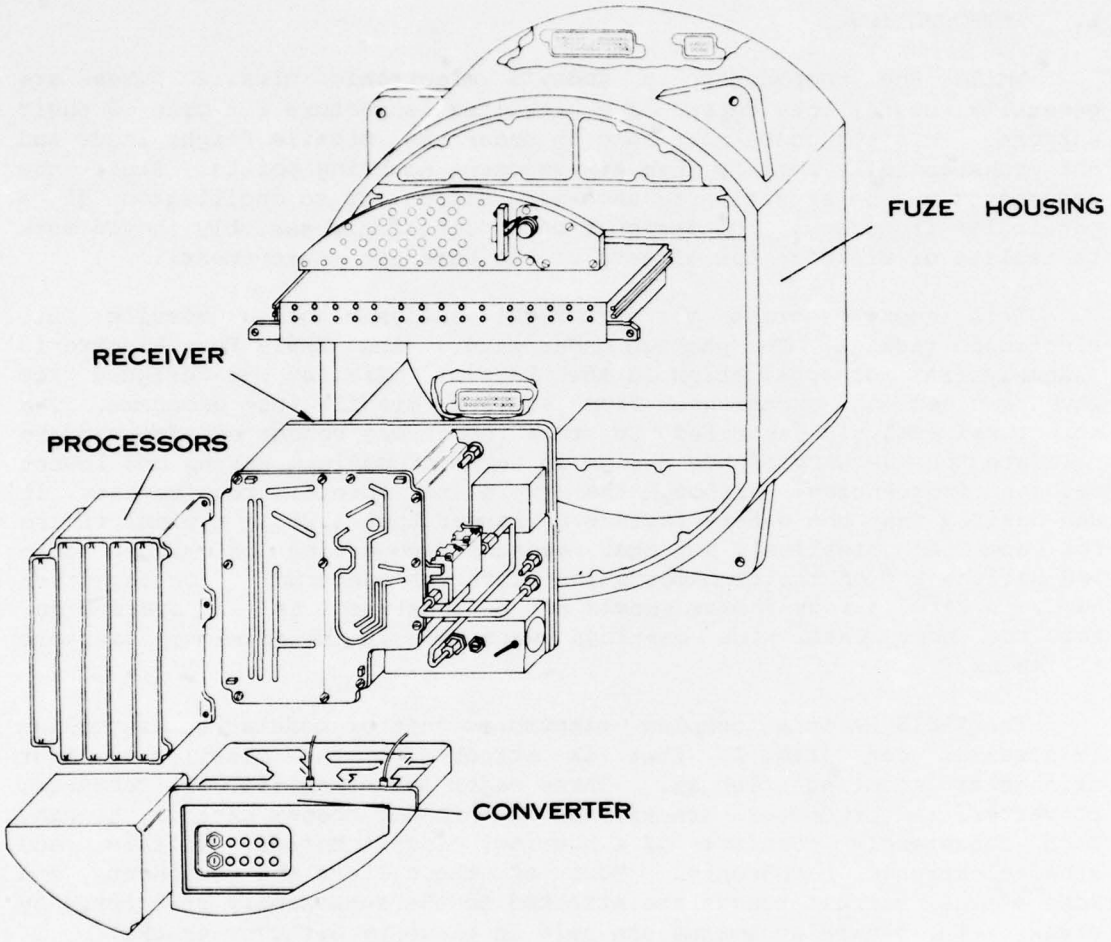

Figure 1. XM818 fuze electronic assembly, exploded view.

The two loading cases investigated were based on measurements and estimates of the missile flight environment.[2] These loadings were

a. a 50-g static acceleration in every direction, and

b. transportation and flight vibration at frequencies from 50 to 3000 Hz. Only the lowest mode shapes and resonant frequencies were computed. Stresses and displacements in vibration were not computed. These depend entirely on the damping of the structural material and any encapsulation used. However, the only accurate source for this information is experimental data. Such an effort was outside the scope of this analysis.

[2] *Environmental Design/Margin Test Plan for XM818 Fuze Type C Electronic Assembly, Code Ident 19202, Part No. 11710921, Harry Diamond Laboratories No. 610-73-03 (October 1973).*

2. APPROACH

The initial step in performing a NASTRAN analysis is to model the structure as a finite mesh of simple geometric elements. The four housings of interest (fuze housing flanges, receiver, converter, and processor) were modeled by quadrilateral and triangular plate elements, and bar elements. The resultant network of elements evolved from an iterative process prescribed by the following guidelines:

a. The elements must conform to NASTRAN programming rules.[1]

b. The combined mesh must nearly resemble the geometry of the structure.

c. Smaller elements are desirable in the regions of large stress gradients to insure sufficient overall accuracy.

d. Smaller elements are also desirable in regions of highest stress to pinpoint the location and magnitude of the maximum stress.

Other inputs to the program were properties of the structural material. The required parameters and their values for A356 aluminum, the alloy from which all of the housings were cast, are listed below.

Properties of A356 aluminum (Permanent cast, T6 condition)[3,4]

Specific gravity = 2.68

Modulus of elasticity = 10.5 (10^6) psi

Modulus of rigidity = 3.95 (10^6) psi

Poisson's ratio = 0.33

Shear strength = 30,000 psi

Tensile strength = 38,000 psi

Tensile yield = 27,000 psi

---

[1] *C. W. McCormick, ed., The NASTRAN User's Manual, NASA SP-222 (October 1969).*

[3] *T. Lyman et al, ed., Metals Handbook, Vol. I, American Society for Metals, 8th ed. (1967).*

[4] *Alcoa Aluminum Handbook, Aluminum Company of America, Pittsburgh, PA (1962).*

Compressible yield = 27,000 psi

Tensile strength at 212°F = 30,000 psi

Tensile yield at 212°F = 25,000 psi

3. DISCUSSION OF INDIVIDUAL STRUCTURES

Once the finite element models had been established, the boundary conditions were specified. Selection was limited to clamped, spring-loaded, or free degrees of freedom in six directions at each point. A discussion of these and other details in the analysis of each structure follows.

3.1 Fuze Mounting Flanges (fig. 2)

The four triangular flanges suspend the 15 lb EA from a mounting ring in the missile structure. Since the wide flanges are relatively stiff in the radial direction, the only significant loading direction is along the missile axis (normal to the flanges). The missile axis direction applies to this structure only; the other two loading directions were not analyzed. The EA housing and its contents were treated as a rigid mass that translates along the missile axis. The four flanges that restrain this motion are two sizes--one pair slightly longer and wider than the other. This difference was ignored, and all four flanges were assumed to be identically large and supporting one-fourth of the EA mass (uniformly distributed along the interfacing edge).

The flanges contact the missile mounting ring on circular bosses--reinforced pads at the end of each flange. Because of the extra thickness and support of these bosses, their circumference was modeled as a clamped (built-in) boundary (fig. 3).

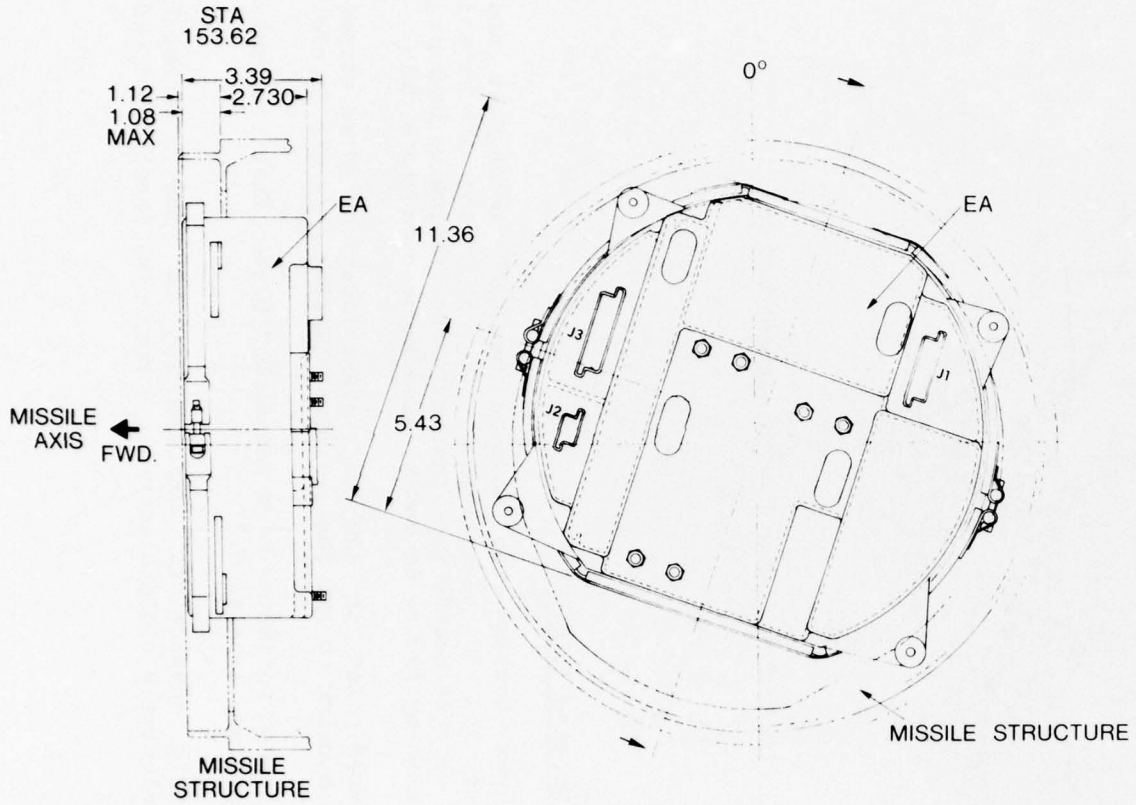

Figure 2. XM818 electronic assembly installed in Patriot missile.

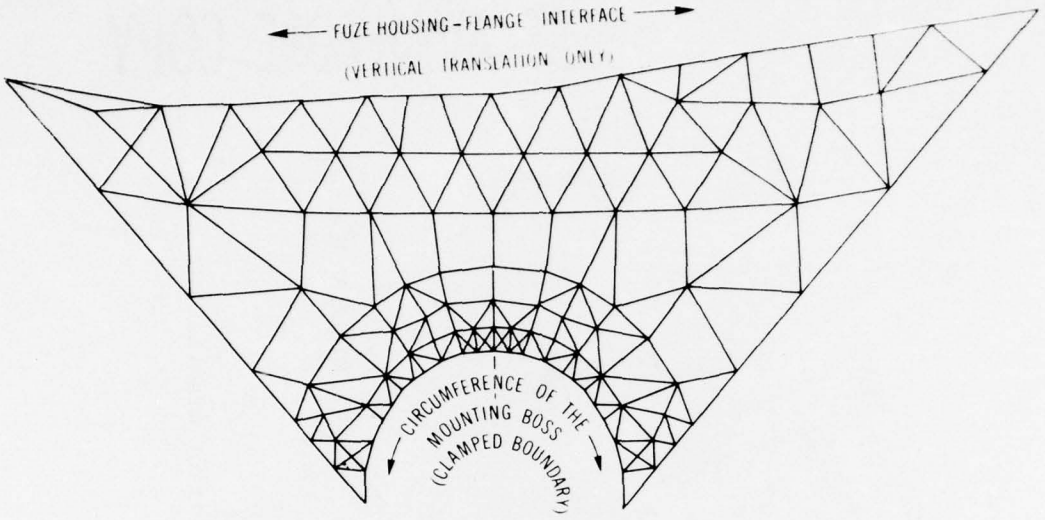

Figure 3. Mounting flange finite element model.

3.2 Receiver Housing (fig. 4)

The receiver housing was modeled by 289 triangular and quadrilateral plates and 50 beam elements (fig. 5). The structural contribution of all circuit boards was ignored. The following boundary conditions, illustrated by figure 6a and b, were imposed on the model:

a. a clamped point at each of eight locations where screws fasten the receiver housing to the fuze housing, labeled A in the figure.

b. the clamped perimeter of a reinforced plate that directly contacts the fuze housing, labeled B.2.

c. geometric constraints corresponding to the attachment points of other relatively rigid electronic components, labeled B.1 and B.3.

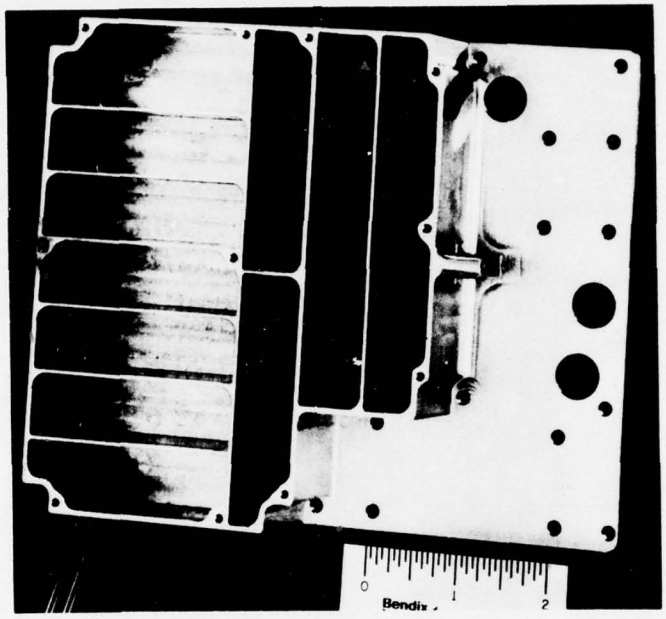

Figure 4. Receiver housing.

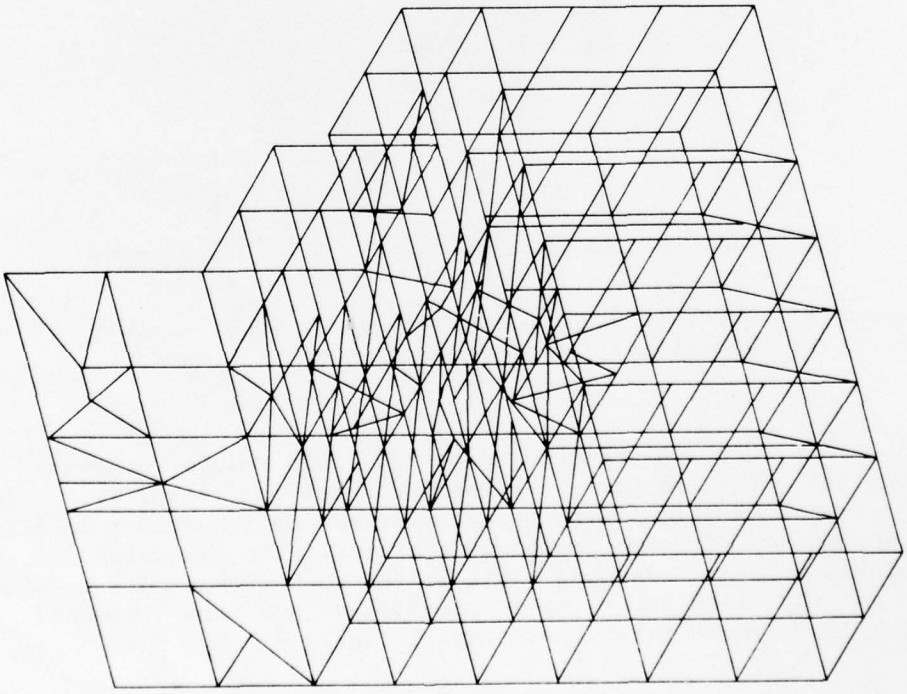

Figure 5. Receiver housing finite element model.

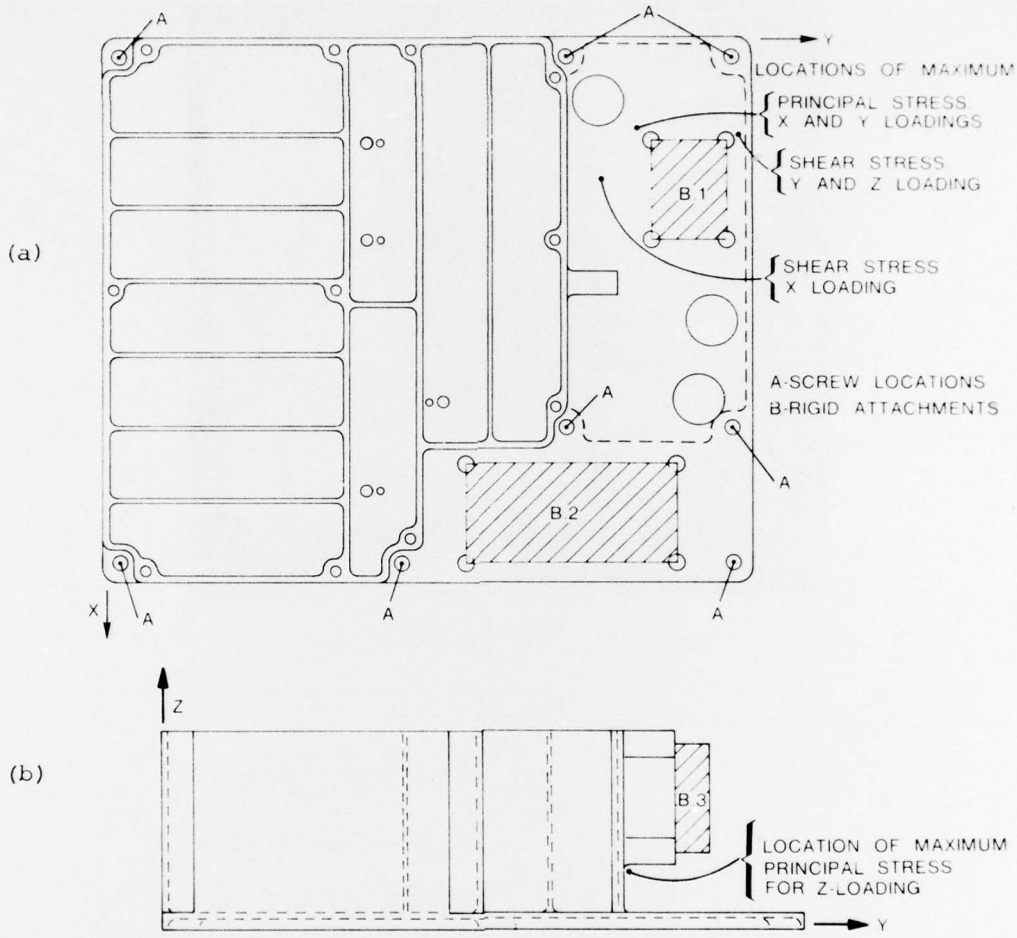

Figure 6. Receiver housing boundary conditions; maximum stress locations: (a) top, (b) side.

This housing was modeled by 29 thin plate elements having five degrees of freedom at each connection (fig. 8). Several simplifications of the housing geometry were made in order to alleviate the programming of some complex features. The exclusion of these difficult-to-program features is believed to have had only a secondary effect on the results. These simplifications are itemized in the following list, which refers to items in figure 9:

a. The recession of plate W and the filter components that mount on it were ignored. Instead, plate W was assumed to be of constant thickness with a continuous midplane.

b. Plate Y was assumed to be so stiff in relation to the rest of the structure that it could be approximated as a rigid body. In other words, no relative displacement was allowed among points attached to it.

c. Once again, the contribution of the circuit boards was ignored. Although the circuit boards undoubtedly contributed significantly to the stiffness of the housing, excluding them cut the problem size in half. However, the simplified analysis became that much more conservative.

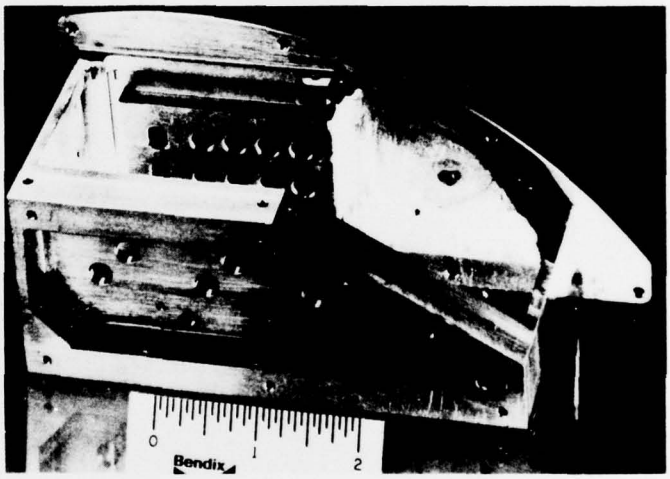

Figure 7. Converter housing.

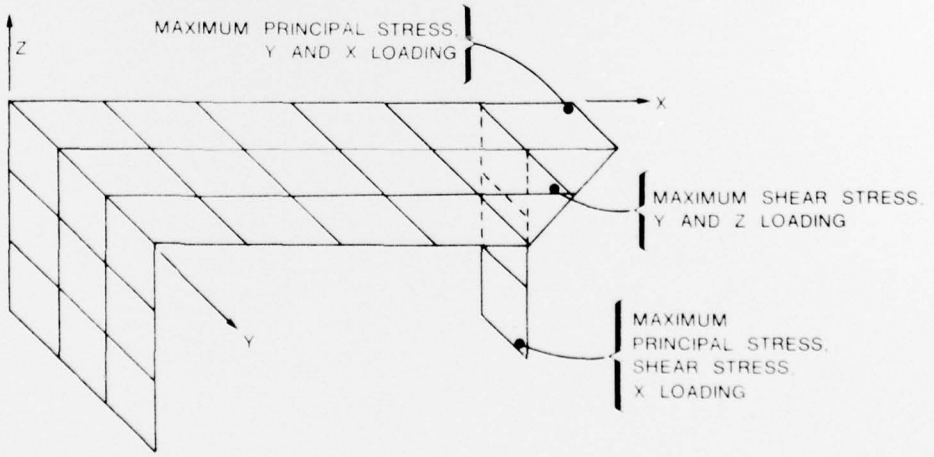

Figure 8. Converter housing finite element model; maximum stress locations.

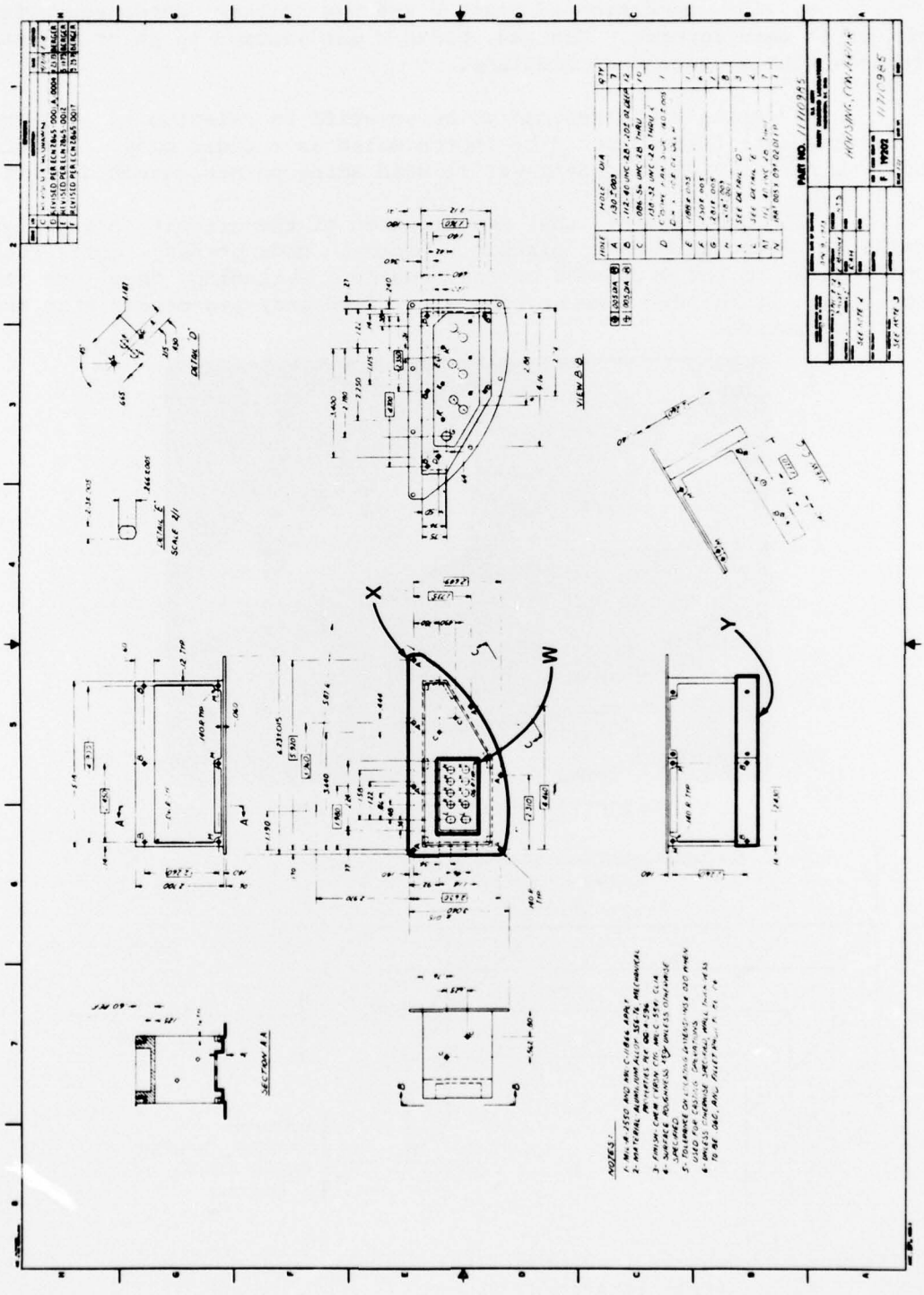

Figure 9. Converter housing simplifications.

The seven mounting screws located on the periphery of plate X (points A, fig. 9) provide the only constrained boundary conditions for the structure. Each of these points was assumed to be clamped.

3.4 Processor Housing (fig. 10)

During examination of the processor housing, it was decided to take advantage of the symmetry and a near-symmetry that exists so as to reduce the size of the model, and thereby simplify the analysis. The processor housing consists of five cells, four that are the same size and the fifth slightly smaller. Additional stiffness is provided by two "straps" that span all five cells. The housing is affixed by screws at each of four corners, with an extra screw at the center of one side. Plane A (fig. 11), perpendicular to and a bisector of each cell, is the only plane of symmetry. The midplane of the center cell, B, is almost another plane of symmetry, except that

a. The odd-sized cell is on only one side.

b. The extra screw location is on the opposite side.

These anomalies were disregarded, and a finite-element model was derived by assuming both planes of symmetry (fig. 12). It was reasoned that the error induced by this idealization would have the effect of increasing the computed stresses, and thus would give a conservative estimate of them. The size of the finite-element model was thereby reduced to a minimum, conserving programming and computing time.

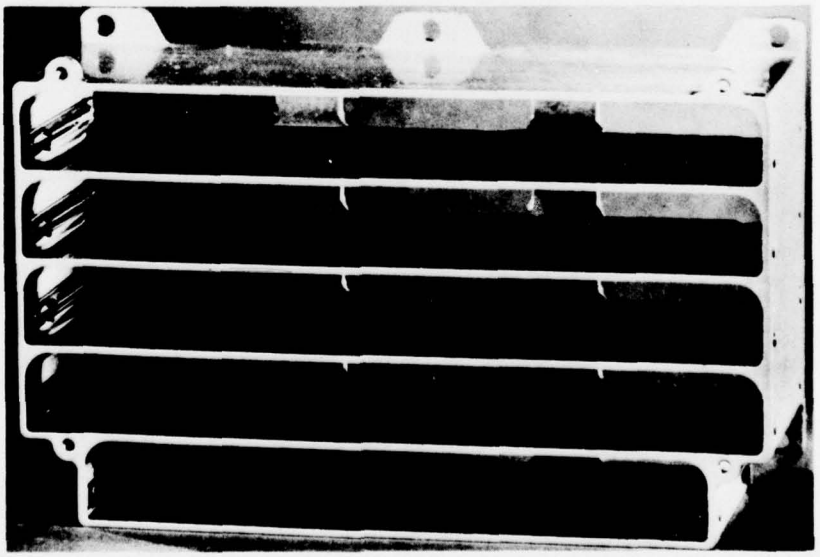

Figure 10. Processor housing.

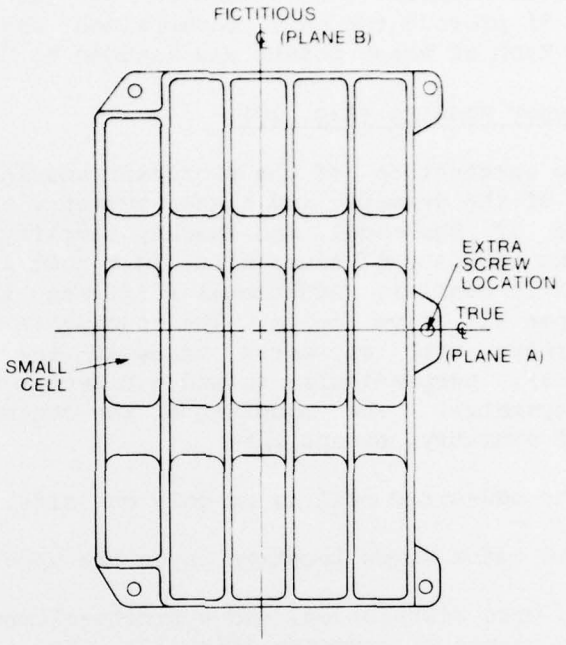

Figure 11. Processor housing: planes of symmetry and pseudo-symmetry.

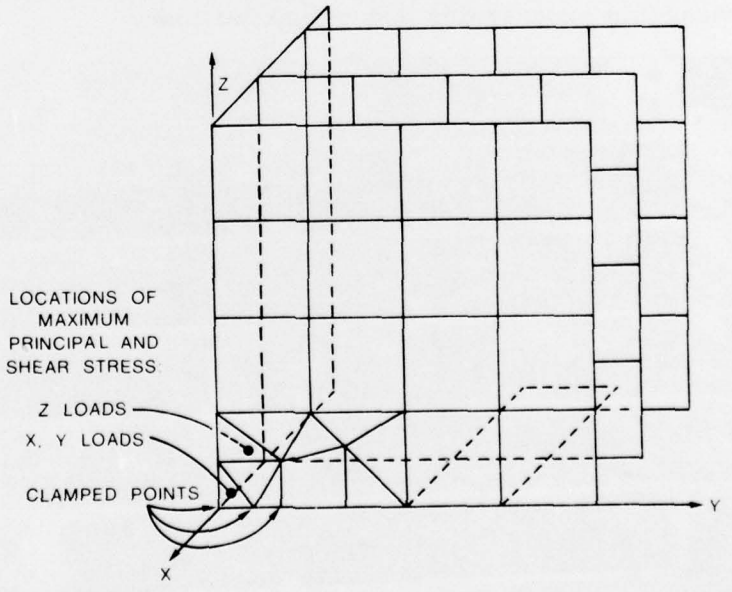

Figure 12. Processor housing finite element model; maximum stress locations.

4. RESULTS

The output of the NASTRAN programs consisted of normal and shear stress distributions, and vibration mode shapes with their corresponding frequencies. The normal and shear stresses were compared to the yield strength of A356 aluminum to arrive at factors of safety. The first few vibration modes of each structure were plotted to determine potentially troublesome mounting locations. A summary appears in table I.

TABLE I. LOWEST RESONANT FREQUENCIES, XM818 FUZE MOUNTING FLANGES AND SUBSTRUCTURES

Structure	Frequency range searched (Hz)	Mode No.	Shape illustrated	Frequency (Hz)
Flanges (fuze)	0-3000	1	fig. 14	1137
Receiver	0-1000	1	fig. 15a	250
		2	fig. 15b	430
		3	Not shown	706
		4	Not shown	969
Converter	0-875	1	fig. 16a	565
		2	fig. 16b	740
		3	fig. 16c	874
Processor	0-435	1	fig. 17	434
	(three others	?	Not shown	531
	found, nos.	?	Not shown	774
	unknown)	?	Not shown	1250

4.1 Fuze Mounting Flanges

The maximum normal stress distribution is shown in figure 13 for the static loading case. A large percentage of the flange area has a maximum normal stress of under 4 kpsi. The highest stress for both loadings occurs in a small region at the boss circumference. Table II summarizes the maximum values of normal and shear stress.

Figure 14 shows the fundamental resonance of the flange mounting, in a mode that occurs at 1137 Hz.

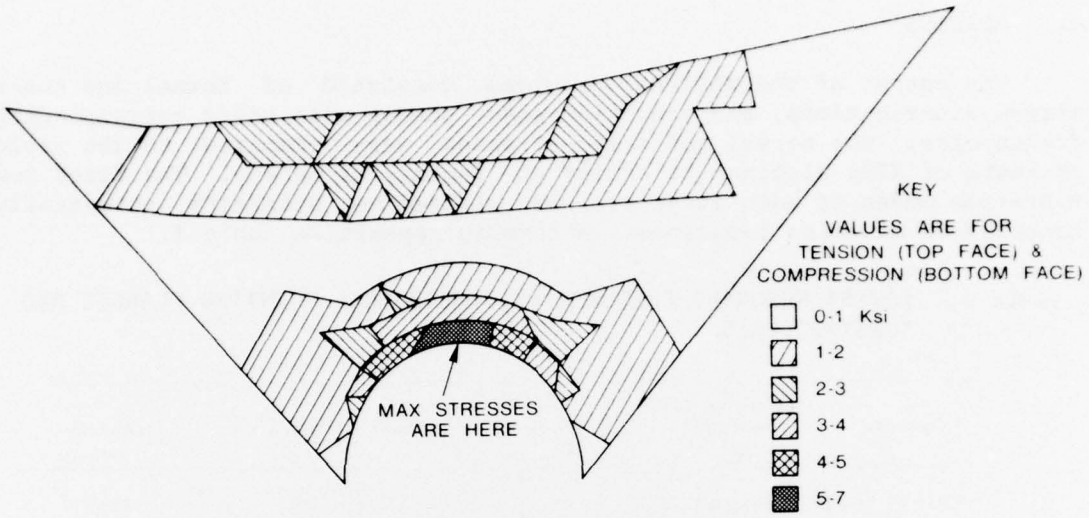

Figure 13. Topographical plot of maximum normal stress--mounting flanges.

TABLE II. SUMMARY OF MAXIMUM STRESSES IN FUZE MOUNTING FLANGE (NORMAL LOAD ONLY)--50 g STATIC LOADING

Maximum principal stress (psi)	6,929
Safety factor* (70°F)	3.90
Safety factor (212°F)	3.61
Maximum shear stress (psi)	2,361
Safety factor (70°F)	12.70

**Relative to yield strength at these temperatures.*

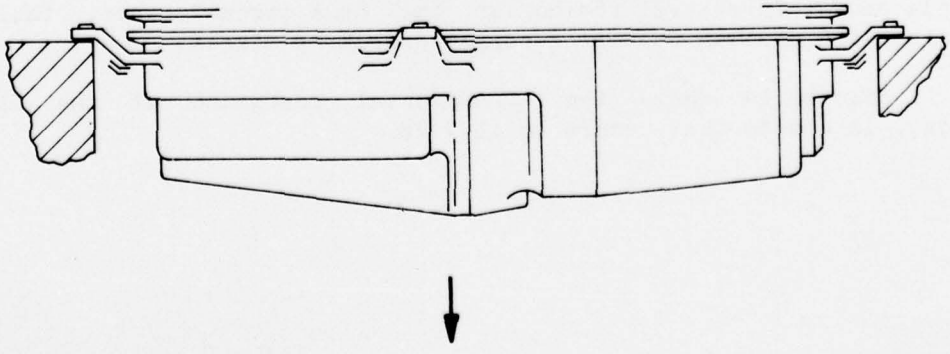

Figure 14. Mounting flanges: mode shape at lowest resonant frequency (1137 Hz).

4.2 Receiver Housing

Preliminary results of the static case indicated that highest stresses occur in the base plate near attachment B.1 and in the wall of the cell supporting attachment B.3 (fig. 6). The finite-element model was revised by modeling these initial areas with a much finer network of plate elements. This revision assured convergence to the maximum values of stress (table III).

The four lowest resonance modes of the receiver housing, two of which are shown in figure 15a and b, all involve oscillation of the same wall. This vibration sensitivity is due to a heavy electronic package that is suspended from supports attached to this wall.

TABLE III. SUMMARY OF MAXIMUM STRESSES IN RECEIVER HOUSING--50-g STATIC LOADING

	Loading parallel to		
	x axis	y axis	z axis
Maximum principal stress (psi)	5,218	5,929	2,287
Safety factor* (70°F)	5.17	4.55	11.8
Safety factor (212°F)	4.79	4.22	10.9
Maximum shear stress (psi)	1,313	1,984	951
Safety factor (70°F)	22.8	15.1	31.5

Relative to yield strength at these temperatures.

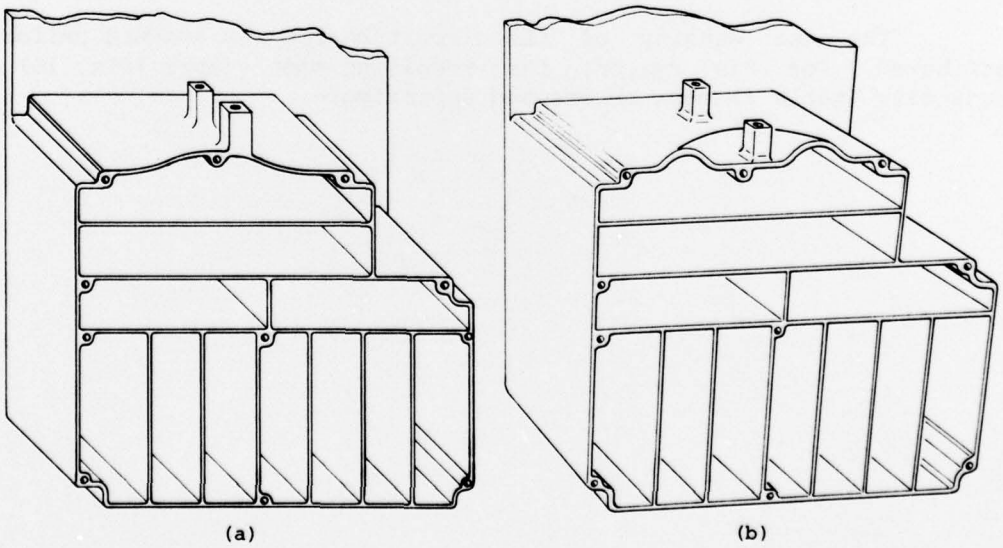

Figure 15. Receiver housing: mode shapes at lowest resonant frequencies: (a) 250 Hz, (b) 430 Hz.

4.3 Converter Housing

The analysis of the static and vibration modes proceeded as described for the receiver housing. The vibration analysis found no resonances of the housing below 1000 Hz. The locations of maximum stress are shown in figure 8. The stress magnitudes and safety factors appear in table IV. The converter was reanalyzed with its three side-mounted circuit boards in place. It was decided to take advantage of a special opportunity afforded by the nature of the circuit board mounts. Because these boards are attached by screws (rather than the Birtcher rails of other boards throughout the EA), the boundary conditions could be accurately modeled. Each screw attachment point was assigned zero degrees of freedom (i.e., clamped).

TABLE IV. SUMMARY OF MAXIMUM STRESSES IN CONVERTER HOUSING--50-g STATIC LOADING

	Loading parallel to		
	x axis	y axis	z axis
Maximum principal stress (psi)	4,769	241	1,213
Safety factor* (70°F)	5.66	112	22.3
Safety factor (212°F)	5.24	104	20.6
Maximum shear stress (psi)	1,775	139	698
Safety factor (70°F)	16.9	216	43

**Relative to yield strength at these temperatures.*

The mass density of the circuit boards was assumed uniformly distributed. For this reason, the resulting mode shapes (fig. 16) and frequencies (table I) must be assumed approximate.

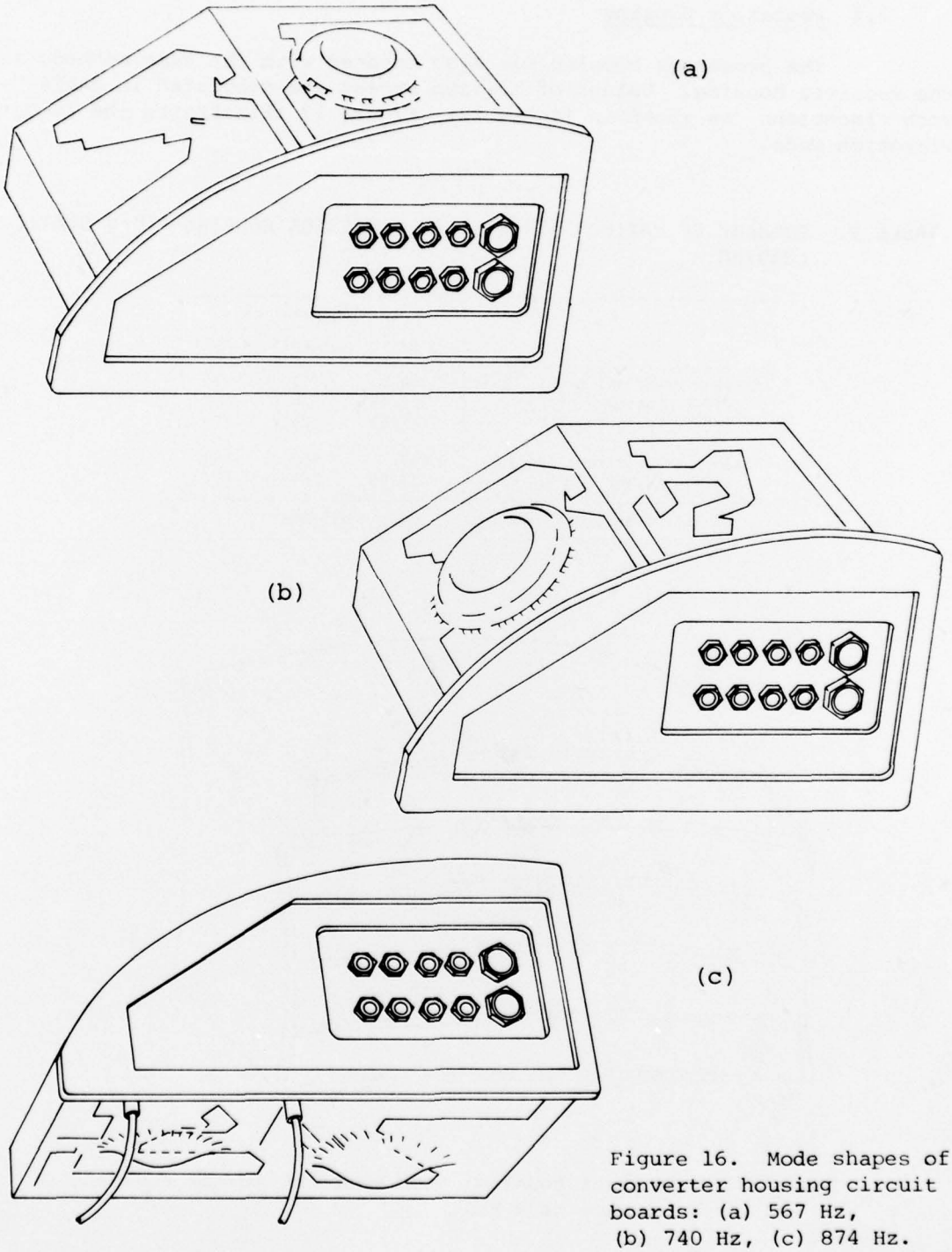

Figure 16. Mode shapes of converter housing circuit boards: (a) 567 Hz, (b) 740 Hz, (c) 874 Hz.

4.4 Processor Housing

The processor housing was also treated with the same methods as the receiver housing. Values of maximum stress are tabulated in table V, with locations as shown in figure 12. Figure 17 illustrates the lowest vibration mode.

TABLE V. SUMMARY OF MAXIMUM STRESSES IN PROCESSOR HOUSING--50-g STATIC LOADING

	Loading parallel to		
	x axis	y axis	z axis
Maximum principal stress (psi)	13,304	1,013	114
Safety factor* (70°F)	2.03	26.7	237
Safety factor (212°F)	1.88	24.7	219
Maximum shear stress (psi)	4,647	550	63
Safety factor (70°F)	6.46	54.5	476

Relative to yield strength at these temperatures.

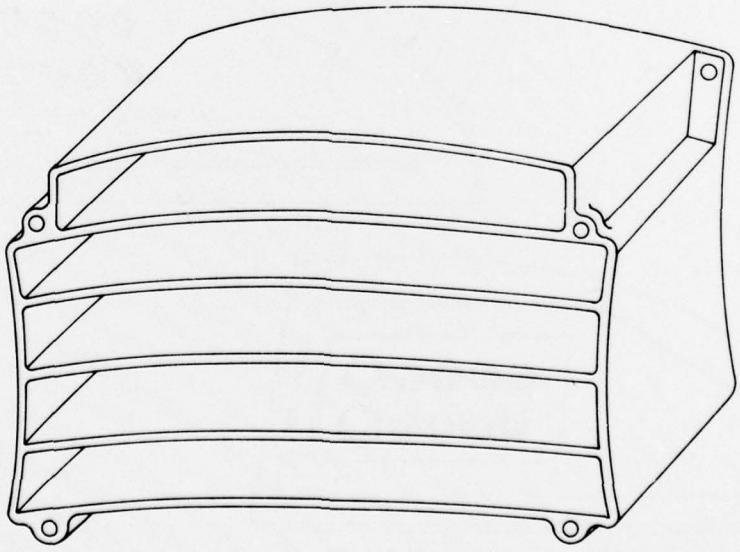

Figure 17. Processor housing: mode shape at lowest resonant frequency (434 Hz).

5. CONCLUSIONS

At a modest level of effort and cost, this NASTRAN analysis yielded significant information about a missile fuze electronic package structure: the weakest areas of the major subassemblies have been pinpointed; the fundamental vibration modes have been found; and the safety factors for static loading have been found to be comfortably large. All this was accomplished in a relatively short time by the use of some time-saving assumptions.

However, the major assumptions imposed several limitations: (1) the stress and displacement levels could not have been computed for vibration and transient loads without adding a significant increase in complexity, (2) the interdependence of the substructures and their mountings in a dynamic loading greatly escalates programming and computing time, and (3) the inclusion of circuit boards and other electronic components, because of their physical complexity, would compound the problem.

DISTRIBUTION

DEFENSE DOCUMENTATION CENTER
CAMERON STATION, BUILDING 5
ALEXANDRIA, VA 22314
ATTN DDC-TCA (12 COPIES)

COMMANDER
USA RSCH & STD GP (EUR)
BOX 65
FPO NEW YORK 09510
ATTN LTC JAMES M. KENNEDY, JR.
CHIEF, PHYSICS & MATH BRANCH

COMMANDER
US ARMY MATERIEL DEVELOPMENT
& READINESS COMMAND
5001 EISENHOWER AVENUE
ALEXANDRIA, VA 22333
ATTN DRXAM-TL, HQ TECH LIBRARY

COMMANDER
USA ARMAMENT COMMAND
ROCK ISLAND, IL 61201
ATTN DRSAR-ASF, FUZE DIV
ATTN DRSAR-RDF, SYS DEV DIV - FUZES

COMMANDER
USA MISSILE & MUNITIONS
CENTER & SCHOOL
REDSTONE ARSENAL, AL 35809
ATTN ATSK-CTD-F

COMMANDER
ARMY MATERIALS & MECHANICS
RESEARCH CENTER
WATERTOWN, MA 02172
ATTN TECH INFO CENTER

COMMANDER
PICATINNY ARSENAL
DOVER, NJ 07801
ATTN SARPA-AD-F,
SYSTEMS ENGR DIV
ATTN SARPA-AD,
FUZE DEV & ENGR DIV
ATTN SARPA-FR,
FELTMAN RESEARCH LAB
ATTN SARPA-TS-T-S,
TECHNICAL LIBRARY

PROJECT MANAGER
PATRIOT PROJECT OFFICE, USARDARCOM
REDSTONE ARSENAL, AL 35809
ATTN DRCPM-MD-T-EG, W. NEWBY (4 COPIES)

COMMANDER
NAVAL SURFACE WEAPONS CENTER
WHITE OAK, MD 20910
ATTN CODE 043, PROJ MGR, FUZES
ATTN CODE 511, MECHANICAL SYSTEMS
MATERIAL DIV
ATTN CODE 730, LIBRARY DIVISION

COMMANDER
NAVAL SHIP R&D CENTER
BETHESDA, MD 20034
ATTN P. MATULA
ATTN G. EVERSTEIN
ATTN J. MCKEE
ATTN M. HURWITZ

DIRECTOR
NAVAL RESEARCH LABORATORY
WASHINGTON, DC 20390
ATTN CODE 2620, TECHNICAL LIBRARY BR
ATTN CODE 5304, MECHANICAL DESIGN

COMMANDER
NAVAL WEAPONS CENTER
CHINA LAKE, CA 93555
ATTN CODE 39, WEAPONS DEPT
ATTN CODE 455, ENGINEERING DIVISION
ATTN CODE 553, PRODUCT DESIGN DIV
ATTN CODE 753, LIBRARY DIVISION
ATTN CODE 75, TECHNICAL INFO DEPT

COMMANDER
NAVAL SURFACE WEAPONS CENTER
DAHLGREN, VA 22448
ATTN ENGINEERING DEPARTMENT
ATTN TECHNICAL LIBRARY

COMMANDING OFFICER
AIR FORCE MISSILE DEV CENTER (MDC)
HOLLOMAN AFB, NM 88330
ATTN LT. R. GUSTAFSON, 6585 TEST GRP (TKO)

DISTRIBUTION

COMMANDER
NAVAL AIR SYSTEMS COMMAND
1411 JEFFERSON DAVIS HWY
ARLINGTON, VA 20360
ATTN NAIR 53233, S. ENGLANDER
ATTN NAIR 53233C, W. ZUKE
ATTN NAIR 53232, A. MCMULLEN
ATTN NAIR 532G2, R. BRITT

DR. J. C. S. YANG
MECHANICAL ENGINEERING DEPT
UNIVERSITY OF MARYALND
COLLEGE PARK, MD 20741

HARRY DIAMOND LABORATORIES
ATTN MCGREGOR, THOMAS, COL, COMMANDER/
FLYER, I.N./LANDIS, P.E./
SOMMER, H./OSWALD, R.B.
ATTN CARTER, W.W., DR., TECHNICAL
DIRECTOR/MARCUS, S.M.
ATTN KIMMEL, S., PAO
ATTN CHIEF, 0021
ATTN CHIEF, 0022
ATTN CHIEF, LAB 100
ATTN CHIEF, LAB 200
ATTN CHIEF, LAB 300
ATTN CHIEF, LAB 400
ATTN CHIEF, LAB 500
ATTN CHIEF, LAB 600
ATTN CHIEF, DIV 700
ATTN CHIEF, DIV 800
ATTN CHIEF, LAB 900
ATTN CHIEF, LAB 1000
ATTN RECORD COPY, BR 041
ATTN HDL LIBRARY (3 COPIES)
ATTN CHAIRMAN, EDITORIAL COMMITTEE
ATTN CHIEF, 047
ATTN TECH REPORTS, 013
ATTN PATENT LAW BRANCH, 071
ATTN GIDEP OFFICE, 741
ATTN LANHAM, C., 0021
ATTN OVERMAN, D., 420
ATTN DAVIS, H., 850
ATTN BARRON, M., 430
ATTN PALMISANO, R., 850
ATTN WESTLUND, R., 620
ATTN LUCEY, G., 910
ATTN MILLER, J., 620
ATTN ANSTINE, C., 620
ATTN BORING, S., 620
ATTN PROBST, M., 640
ATTN FRYDMAN, A., 850
ATTN CURCHACK, H., 850
ATTN FONOROFF, B., 0021
ATTN NEILY, D., 0021 (10 COPIES)
ATTN CRAWLEY, J., 610